References

Born M and Wolf E 1980 *Principles of Optics* 6th edn (Oxford: Pergamon) pp 24–32

Dekkers H P J M, Moraal P F, Timper J M and Riehl J P 1985 Optical artifacts in circularly polarised luminescence spectroscopy
Appl. Spectrosc. **39** 818–21

Ditchburn R W 1976 *Light* 3rd edn (London: Academic)

Gooch C H and Tarry H A 1975 The optical properties of twisted nematic liquid crystal structures with twist angles $\leqslant 90°$
J. Phys. D: Appl. Phys. **8** 1575–84

Raynes E P and Tough R J A 1985 The guiding of plane polarised light by twisted liquid crystal layers
Mol. Cryst. Liq. Cryst. Lett. **2** 139–45

Shurcliff W A 1962 *Polarised Light* (Cambridge, MA: Harvard University Press)

Tarry H A 1975 *SERL Technical Memorandum* no 951 (unpublished data)

J. Phys. E: Sci. Instrum. **20** (1987). Printed in the UK

A high-temperature dilatometer using optical heterodyne interferometry

Masahiro Okaji and Hidetaka Imai
National Research Laboratory of Metrology, 1-1-4, Umezono, Sakuramura, Niiharigun, Ibaraki 305, Japan

Received 14 September 1986, in final form 3 November 1986

Abstract. A high-precision interferometric dilatometer developed for use at high temperatures is described. The dilatometer consists of a double-path laser interferometer with optical heterodyne interferometry and a radiant heating furnace, which provides high accuracy length measurement and rapid heating and cooling for the specimen. The uncertainty in length measurement by the newly developed dilatometer is estimated to be within 2 nm in the range between room temperature and 1100 K.

1. Introduction

Recently, the accurate determination of the thermophysical properties of various solid materials at high temperatures has been particularly required with the development of new materials such as heat-resistant alloys, glasses and ceramics.

At high temperatures, various measuring methods such as the push-rod dilatometer, the twin telemicroscope method and the Fizeau interferometer have been commonly used until now. All these methods are structurally simple, reliable, and easy to treat but they do have a few limitations. In the case of a push-rod dilatometer, the measurement is not accurate enough and requires calibration by the absolute method. The twin telemicroscope method is absolute and non-contacting, but the sensitivity in length measurement is insufficient (the resolution of the system is about 1 μm at the most), and automation is difficult. In the case of Fizeau interferometry, the DC level of interference fringes could be affected by thermal radiation from the specimen or the reduction of the intensity of the reflected beams. The main reasons for the intensity reduction are the adsorption of evaporating mist, e.g. oil from the mechanical pump, to the inside of the optical window of the vacuum furnace, and the optical misalignment caused by the thermal deformation in the system. Consequently, the change in DC level increases an uncertainty in the fringe determination, and reduces the accuracy of the length measurement. In contrast, the detection method using AC fringe fractions is not affected by a change of DC level. Therefore, optical heterodyne interferometry (the AC fringe detection method) should be an especially suitable method for high-temperature dilatometry.

This paper describes an application of the interferometric method to high-temperature dilatometry. The double-path interferometer, which has been developed previously, is combined with the radiant heating furnace to achieve both precise and efficient measurement of thermal expansion coefficients.

2. Design of the apparatus

2.1. Interferometer

For achieving high resolution in the measurement of linear

0022-3735/87/070887 + 05 $02.50

thermal expansion coefficients, a double-path interferometer utilising optical heterodyne interferometry has been developed. The details of the interferometer have been reported previously (Okaji and Imai 1984). The AC fringe detection method is highly sensitive in length measurement and the determination of the fringe fraction can be achieved to better than 2 nm.

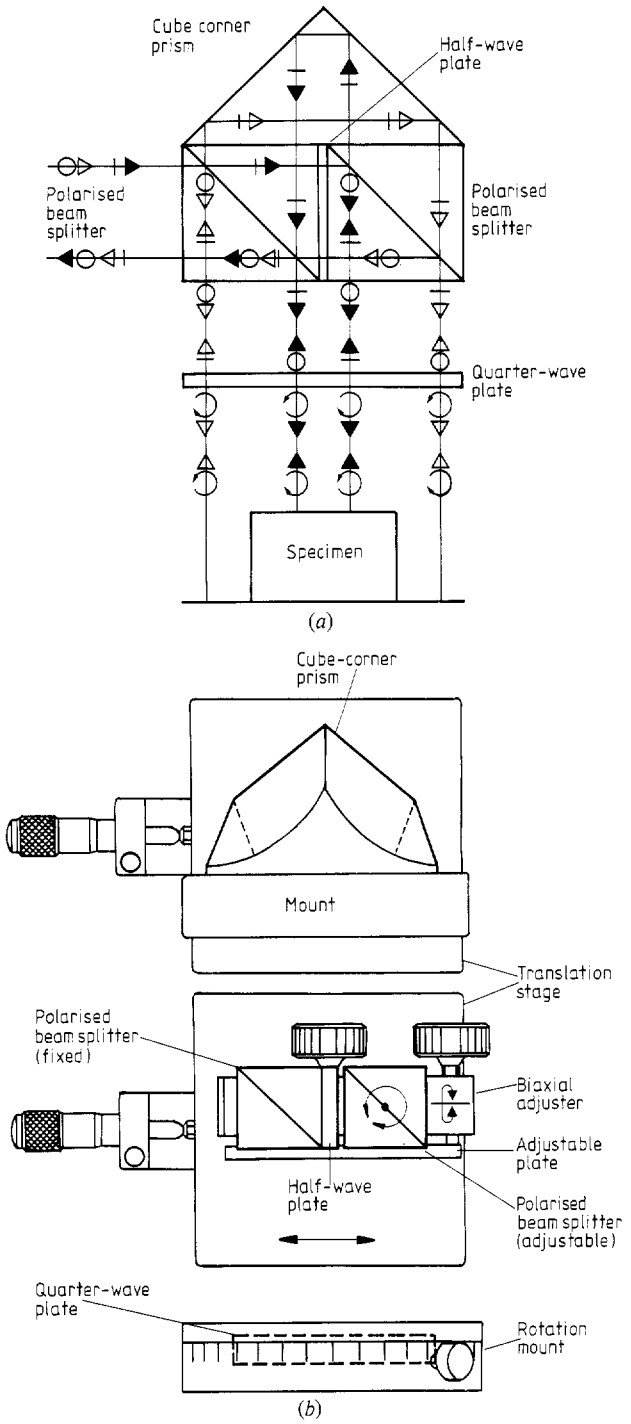

Figure 1. The double path interferometer. (*a*) Schematic design of the optical configuration. (*b*) Mechanical arrangement. The upper and lower translation stages are used for the adjustment of the positions of the cube-corner prism and the two polarised beam splitters, respectively. The biaxial adjuster is used to rotate or tilt one of the polarised beam splitters.

A schematic diagram and a mechanical arrangement of the interferometer are shown in figure 1(*a*) and (*b*) respectively. The interferometer consists of five optical components, i.e. two polarising beam splitters, a cube-corner prism, a half-wave plate and a quarter-wave plate. Each component is mounted on the fine mechanical adjuster to achieve fine optical alignment so that optimum interference fringes can be easily obtained by adjusting the angle between the two polarising planes of the beam splitters. Arrows in figure 1(*b*) show the adjustment directions of the optical elements. In addition, specimens of different sizes can be

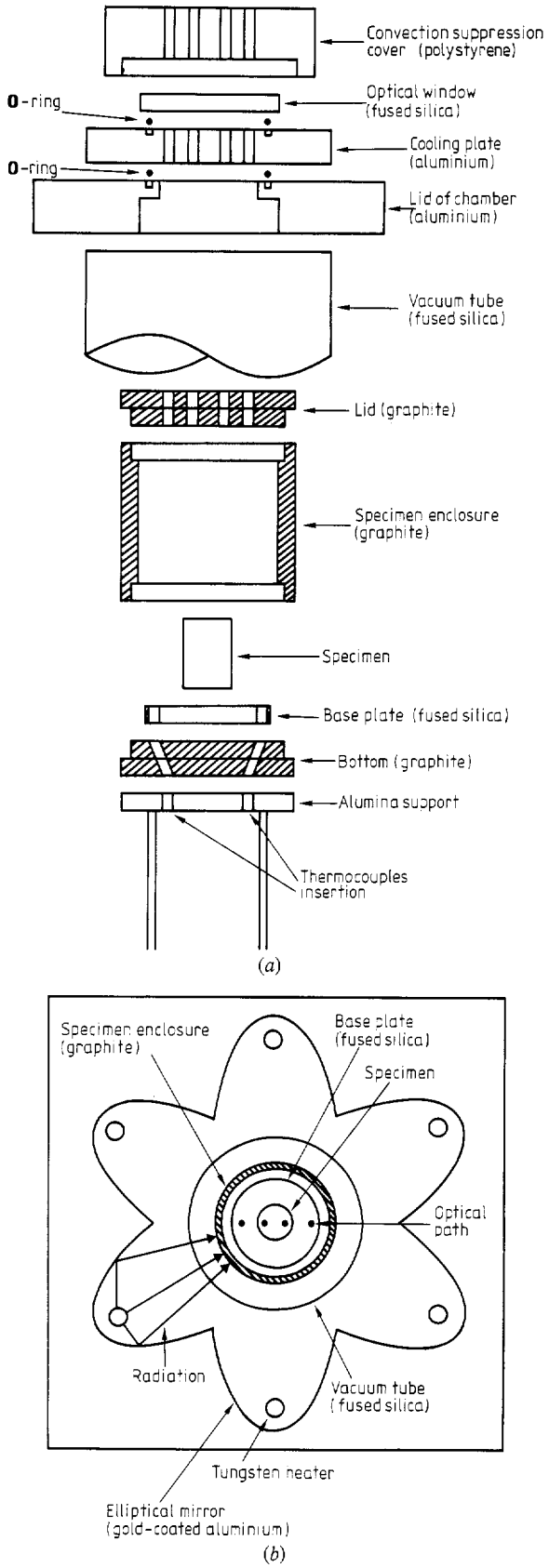

Figure 2. The image furnace and the specimen system. (*a*) Vertical cross section. Specimen set-up detail. (*b*) Horizontal cross section.

measured by adjusting the distance between the beams of the interferometer. The incident beam and reflected beam of the interferometer are maintained parallel to prevent any optical misalignment caused by the deformation of the system (Okaji and Imai 1985). This provides not only a high accuracy in length measurement but also wide tolerance to the specimen shapes and dimensions. Furthermore, the specimen set-up time would be shortened. The size of a specimen is nominally 20 mm long and 15 mm in diameter, both ends of which are polished to have a flatness of less than one-tenth of a wavelength.

Generally, the two mirrors can be a few seconds out of true, whilst still obtaining sufficiently clear interference fringes for usual interferometers, such as the Fizeau method. On the other hand, the double-path interferometer has wide tolerance to the non-parallelism depending on the distance between the interferometer and the specimen system and the diameter of the optical beam. The distance and the diameter are 0.5 m and 4 mm for the present system. The tolerance is measured to be ± 400 seconds of arc ($\cong 0.1°$) under the condition that the amplitude of the AC interference fringe comes to half of the maximum value and this figure agrees well with the calculated one.

2.2. *Furnace*

A radiant heating furnace is used in this system for achieving very rapid heating and cooling of the specimen system. A vertical and a horizontal cross section of the furnace and the specimen enclosure are shown in figure 2(*a*) and (*b*). The furnace consists of a symmetrical configuration of six gold coated elliptical mirrors which are made of aluminium alloy and cooled by water. Every mirror has a tungsten heater at one of its focal points, and the radiation from which is reflected toward the other focal point, i.e. the furnace centre. Because of the low thermal mass of the furnace, a very rapid response of the specimen temperature can be achieved.

The specimen supporting system is set up in an evacuated transparent fused-silica tube. The specimen is put on a fused silica optical flat (30 mm diameter × 5 mm thickness), on which gold is deposited and it is held on a graphite support. The specimen and the base plate are set up in a graphite enclosure, whose thickness is about 10 mm. The reason for using the graphite enclosure is to obtain sufficient temperature uniformity by means of its good thermal conductivity and high-absorption of the heat radiation. The temperature distribution in the enclosure is confirmed to be within ± 0.5 K at 1100 K, and it is much smaller at lower temperatures. The temperature of the specimen is measured by high-precision R-type thermocouples. The thermocouples are inserted from the bottom of the enclosure to avoid being heated directly, which can reduce the temperature distribution of the specimen system.

The response time of the specimen temperature change is very short compared with that of a usual vacuum furnace which normally consists of a coiled heater and a thick thermal insulator. The typical conditioning time of the specimen to reach thermal equilibrium after the temperature rise of 100 K in the furnace is about 2 h at 350 K, 1 h at 550 K, 30 min at 750 K, 25 min at 1000 K, and 15 min at 1300 K, respectively.

2.3. *Data aquisition system*

The optical and electrical arrangement of the measuring system is shown in figure 3. A 2 mW two-frequency Zeeman stabilised laser is used as an optical source. The phase difference of the

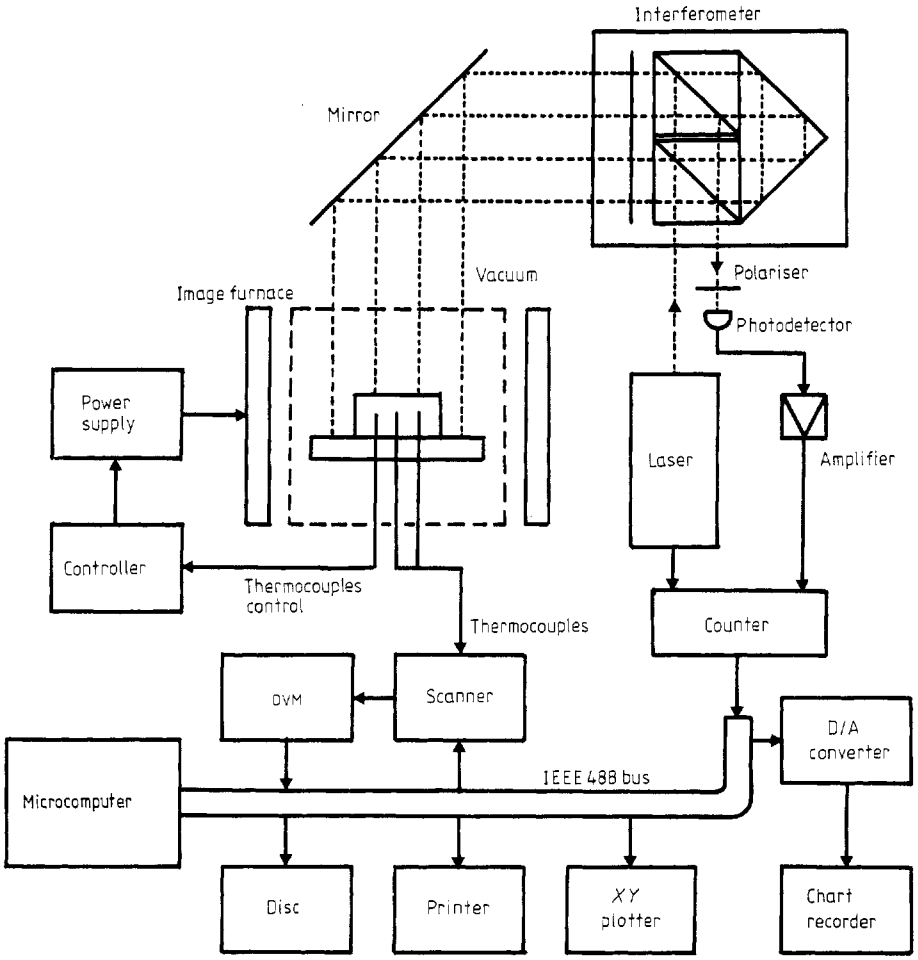

Figure 3. The optical and the electrical arrangement of the measuring system.

reference beat signal and the interference beat signal, which corresponds to an AC fringe fraction, is measured by a universal counter. The temperature of the furnace is controlled to a certain temperature between room temperature and 1300 K by the programmable temperature controller, which can create any pattern of a temperature heating/cooling ratio and holding time. All data aquisition is accomplished by a microcomputer with the IEEE-488 interface bus. The temperature data from the thermocouples and the fringe fraction data from the interferometer are read, analysed and stored on a disc system and recorded by a printer, an X–Y plotter, and a chart recorder.

3. Performance of the dilatometer

In order to confirm the performance of the dilatometer, the stability of the fringe determination was examined at several temperatures. The fluctuation of the fringe fraction is caused mainly by the variation of the refractive index of the air along the optical paths. In the case of the radiant heating furnace, the required input energy to raise the temperature in the furnace is relatively small compared with the usual furnace, so that it reduces the thermal disturbances to the interferometric system. The determination of the AC fringe fraction is accomplished by the universal counter with a 30 ms gate time and averaged 100 times to obtain a better resolution in length measurement. The long term stability of the interferometer is confirmed to be within 1 nm (1/600 of a wavelength) over 10 h. As is shown in figure 4, the fluctuation of the fringe fraction is negligibly small at temperatures below 600 K. It increases gradually with the temperature rise, but is still of the order of 1 nm at 1100 K.

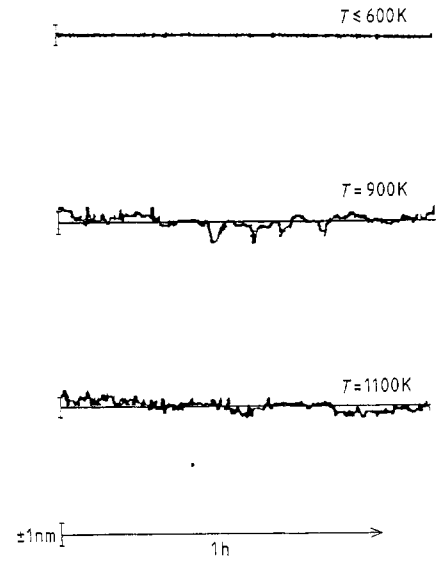

Figure 4. Temperature dependence of the fringe determination.

If there is some temperature variation in the optical window, it produces the zero drift of fringe fraction. To reduce this uncertainty, the optical window, which is made of an antireflection coated fused-silica parallel plate (30 mm diameter and 8 mm thick), is maintained at the constant temperature by an aluminium plate which is cooled by water (see figure 2(*a*)). The zero drift of the fringe fraction is then investigated by raising the furnace temperature with no specimen on the base plate. In this case, all four beams from the interferometer are reflected by the base plate. The measured results are shown in figure 5. Full circles represent the zero drift without the cooling plate of the optical window, and open circles represent the drift with the cooling plate. It is clear that the amount of fringe

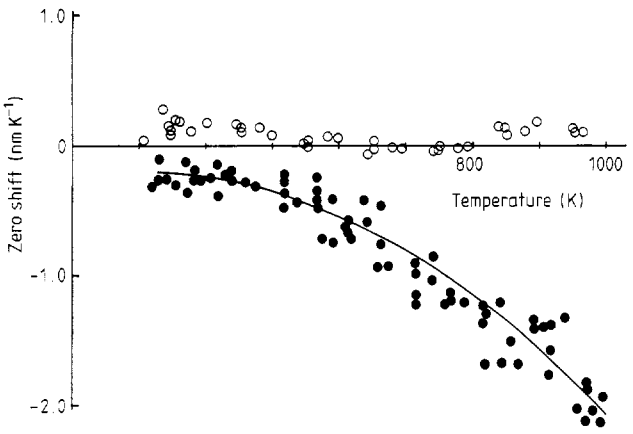

Figure 5. Zero-drift of the fringe fraction against furnace temperature. Open circles, with the cooling plate; full circles and curve, without the cooling plate.

movement is reduced remarkably as an effect of the cooling plate. From the above result, the zero drift can be suppressed to within 5×10^{-11} m K^{-1}.

The performance of the dilatometer is estimated from each of the error sources, such as, the long term stability of the laser wavelength (1×10^{-9}), the fringe determination (2 nm (1/300 of wavelength)), the uncertainty of the zero-drift of the fringe fraction (5×10^{-11} m K^{-1}), the temperature determination of the specimen (0.25 K) and the temperature calibration error (0.3 K). The error sources and the estimated values of uncertainty for a 20 mm long specimen over a 50 K temperature interval are summarised in table 1. The total uncertainty of the system is estimated to be

$$[(0.21 \times 10^{-16}) + (5 \times 10^{-5})\alpha^2]^{1/2} + (6 \times 10^{-3}) \mid \alpha \mid K^{-1}.$$

Here, α represents the linear thermal expansion coefficient. The total uncertainty is calculated to be 1.4×10^{-8} K^{-1} (6.6×10^{-8} K^{-1}) for a material whose thermal expansion coefficient is 10^{-6} K^{-1} (5×10^{-6} K^{-1}).

Table 1. Sources and estimated values of uncertainty for a 20 mm long specimen over a 50 K temperature interval.

Source	Contribution to expansion coefficient (K^{-1})
Laser wavelength stability	2×10^{-11}
Fringe determination	2×10^{-9}
Zero drift of fringe fraction	2.5×10^{-9}
Temperature determination	$5 \times 10^{-3} \times \alpha$
Thermocouple calibration	$6 \times 10^{-3} \times \alpha$
Total	$[(0.21 \times 10^{-16}) + (5 \times 10^{-5}) \times \alpha^2]^{1/2} + (6 \times 10^{-3}) \mid \alpha \mid$

4. Summary

The design and performance of the high-temperature interferometric dilatometer are described. The double-path interferometer with the AC fringe detection method involves both high sensitivity in length measurement and versatility with the specimen preparation and set-up. The radiant heating furnace provides an efficient measurement and specimen turnaround time through rapid heating and cooling of the specimen system. The dilatometer is capable of thermal expansion measurement in the temperature range from room temperature to 1100 K. The

uncertainty in the length measurement for the above temperature regions is estimated to be better than 2 nm.

International collaboration between the National Research Laboratory of Metrology, Japan and the National Physical Laboratory, UK is now helping evaluate the accuracy and performance of the interferometric dilatometer by using the present measuring system and a similar measurement system at NPL.

References

Okaji M and Imai H 1984 A practical measurement system for the accurate determination of linear thermal expansion coefficient
J.Phys. E: Sci. Instrum. **17** 669–73

Okaji M and Imai H 1985 Precise and versatile systems for dilatometric measurement of solid materials
Precision Engng **7** 206–10

J. Phys. E: Sci. Instrum. **20** (1987). Printed in the UK

Optical inspection and monitoring of crazing in enamelled wires using light scattering

I F Faria Jr†, L C M Miranda‡, H Vargas§ and E Fernandes‖
† Centro Técnico Aeroespacial, Instituto de Estudos Avançados, 12200 São José dos Campos, São Paulo, Brazil
‡ Ministério da Ciência e Tecnologia, Instituto de Pesquisas Espaciais, Laboratório Associado de Sensores e Materiais, Caixa Postal 515, 12201 São José dos Campos, São Paulo, Brazil
§ Universidade Estadual de Campinas, Instituto de Física, 13100 Campinas, São Paulo, Brazil
‖ Pirelli SA, Centro de Engenharia de Cabos, 09000 Santo André, São Paulo, Brazil

Received 30 April 1986, in final form 12 November 1986

Abstract. A new method is proposed for the inspection and monitoring of micro-defects in enamelled wires. The method is based on the measurement of the light scattered from the wire. Its advantages over conventional optical and scanning electron microscopy are also discussed.

1. Introduction

During the manufacturing process of enamelled wires and electrical appliances, wire is subjected to different types of deformation and chemical environment. As a result of these processes some defects like craze will appear in the bulk polymer as a way of stress relaxation, thereby decreasing the dielectric strength of the enamelled wire and affecting the electrical performance of the appliances. Needless to say, the identification as well as the study of the mechanisms responsible for the development and propagation of these damaged regions are of the utmost importance to the industry. The observation of craze in enamelled wires has been done so far with conventional optical and scanning microscopes (Basin and Artemova 1978). These methods are slow, require some sample preparation and difficult to adapt to an on-line quality control unit. In particular, in the case of the scanning electron microscope the incident electron beam can generate some extra defects that may lead to erroneous information about the original defects.

In this paper, we describe a new method for inspecting and monitoring the wire coating. It is based on the change in the intensity of the scattered light from the wire as an incident light beam crosses the damaged region. Since this technique does not require any contact with the material being tested it is suitable for the development of an on-line inspection device. Light scattering techniques similar to the one described below have been used successfully for a long time as an inspecting technique in several systems, such as the detection of pinholes on translucent substrates and the inspection of ceramic surfaces, laser Doppler velocimeters (Elion 1967) and laser ultramicroscope (Vand *et al* 1966). For a review of the scattering techniques applied to process monitoring we refer to the work by Charschan (1972). In the context of the utility industry Cheo (1986) has reported the development of a similar laser

0022-3735/87/070891 + 03 $02.50